14 Nov 1992

Classical Description And Calculation Of Ionization In Collisions Of 100 Ev Electrons And Positrons With He And H2

D. R. Schultz

L. Meng

Ronald E. Olson
Missouri University of Science and Technology, olson@mst.edu

Recommended Citation

D. R. Schultz et al., "Classical Description And Calculation Of Ionization In Collisions Of 100 Ev Electrons And Positrons With He And H2," *Journal of Physics B: Atomic, Molecular and Optical Physics*, vol. 25, no. 21, pp. 4601 - 4618, IOP Publishing, Nov 1992.
The definitive version is available at https://doi.org/10.1088/0953-4075/25/21/024

Journal of Physics B: Atomic, Molecular and Optical Physics

Classical description and calculation of ionization in collisions of 100 eV electrons and positrons with He and H_2

To cite this article: D R Schultz *et al* 1992 *J. Phys. B: At. Mol. Opt. Phys.* **25** 4601

J. Phys. B: At. Mol. Opt. Phys. 25 (1992) 4601–4618. Printed in the UK

Classical description and calculation of ionization in collisions of 100 eV electrons and positrons with He and H_2

D R Schultz†, L Meng and R E Olson

Laboratory for Atomic and Molecular Research and Department of Physics, University of Missouri-Rolla, Rolla, MO 65401, USA

Received 11 May 1992, in final form 11 August 1992

Abstract. In order to explore the range of applicability of the classical trajectory Monte Carlo technique concerning the phenomena associated with light-particle impact of atoms and molecules, we present calculations of the singly and doubly differential cross sections for 100 eV electron and positron impact of He and H_2. Through comparison with experimental measurements it is noted in what regimes of ejection energy and angle the classical model describes reasonably the process of ionization by electrons. We find that reasonable agreement is obtained regarding the integrated (singly differential and total) cross sections, while the features of the doubly differential cross section which evidently come about due to quantum mechanical aspects of the collision are not reproduced. In these instances the classical cross sections reflect an averaging over electron angles and energies of the observed doubly differential cross sections. Difficulties associated with the classical model of the many electron atom which arise specifically in light-particle impact are discussed as well as a comparison with a distorted wave Born approximation for electron impact of helium.

1. Introduction

Electron impact ionization of atoms, molecules and ions is a ubiquitous phenomenon. Its elucidation is a fundamental goal of atomic collision physics as well as a practical tool for plasma physics, solid state physics and astrophysics. In addition, much has been learned theoretically about the process of ionization by light-particle impact by considering analogous collisions involving impinging positrons. Relatively recently, positron sources which are low in energy, monoenergetic and well collimated have been developed and now play an important role in experiment, and complement the more traditional electron impact studies (see the recent reviews by Kauppila and Stein 1989, Charlton and Laricchia 1990, Schultz *et al* 1991).

In particular, it is of great interest to probe the range of applicability of various theoretical approaches which seek to treat such phenomena. In this work we wish to find to what extent intermediate energy light-particle–atom collisions may be described by a model utilizing classical particle trajectories and a statistical, quasi-quantal distribution representing the initial state. A strenuous test of this model, the classical trajectory Monte Carlo (CTMC) method, is the calculation of singly and doubly differential cross sections for the ejection of electrons by electron or positron

† Present address: Physics Division, Oak Ridge National Laboratory, Oak Ridge, TN 37831-6373, USA.

0953-4075/92/214601+18$07.50

impact. Experimental determinations of this quantity exist for electron impact of helium and molecular hydrogen and serve as the basis for our comparison. Very recently Shyn (1992) has published doubly differential ionization cross sections for electron impact of atomic hydrogen. Comparison of this fundamental measurement with CTMC calculations will be the subject of a forthcoming study.

A large number of works over the past two decades have shown the classical trajectory Monte Carlo method to be a powerful and useful technique for the description of especially ionization and charge transfer in intermediate energy ion–atom collisions. (Intermediate energies correspond to collisions in which the projectile velocity is on the order of the electronic orbital velocity.) Shortly after its introduction by Abrines and Percival (1966a, b) to describe proton–atomic hydrogen collisions, these authors considered electron impact (Abrines *et al* 1966) and positronium formation in collisions with atomic hydrogen (Percival and Valentine 1967). However, a robust test of the method was hampered by the lack of comprehensive experimental data regarding differential cross sections for electron impact ionization and for positronium formation, and due to the substantial computational effort required to produce enough trajectories to obtain good statistics in the Monte Carlo simulation for differential cross sections. The method was later applied by Percival (1973, 1974) to the calculation of energy transfer cross sections for the collisions of electrons with atoms and by a number of authors to explore the threshold behaviour of the ionization total cross section for comparison with the Wannier model (Boesten *et al* 1976a, b, Dimitrijevic and Grujic 1979, 1983, Wetmore and Olson 1986). The behaviour of the total cross section for light-particle impact of H, He^+ and He for larger impact energies was studied as well by Banks and Boesten (1978), Percival and Richards (1978), Ohsaki *et al* (1985), Schultz and Olson (1989), Schultz (1989) and Schultz *et al* (1989). Cross sections differential in the angle and energy of the electrons were obtained by Banks and Boesten (1978) and detailed doubly differential cross sections were recently calculated by Olson and Gay (1988) and by Schultz and Reinhold (1990) for 100 eV positrons colliding with atomic hydrogen.

Thus, with the advent of computing resources sufficient for the calculation of the millions of trajectories necessary to compute differential ionization cross sections, it is timely to compare the CTMC model results to the existing experimental measurements. In addition, such a study is relevant since in the intermediate energy regime the classical description of the electron removal process is most valid. This is because the interaction is strong and highly non-perturbative, and since many reaction channels are open and the interference of only a few is not expected to lead to radically quantum mechanical behaviour. Quantum tunnelling, for example, is not expected to contribute appreciably in the present intermediate energy collisions, except perhaps to some extent in certain specific ejection regimes such as those arising from very glancing collisions in which the classical model of the atom is more stable against small perturbations than the quantum mechanical model. In fact, in this regime the leading quantum mechanical corrections to the classical behaviour seem to enter primarily through the initial conditions, which the initial ensemble distribution is incorporated to mimic, and the evolution in the collision is largely classical. Essentially for these same reasons this is also a difficult regime to access by quantum mechanical approximation, i.e. a prohibitively large basis set is required in coupled channels approximations and the energy is too low to be treated with complete accuracy by perturbative approximations. These observations form the basis of the success and utility of the CTMC approach.

After a brief description of the specific CTMC models utilized in this work (section 2), we present total cross sections as a function of impact energy compared to experimental data for electron and positron impact of H, H_2 and He, as a benchmark for the results of the differential cross section calculations. Next, in section 3, comparison is made with the available experimental measurements concerning ionization cross sections differential in both the electron angle and energy (singly differential cross sections) for 100 eV electrons and positrons colliding with He and H_2. Finally, as the most strenuous test we present doubly differential cross sections for these collision systems compared with various experimental measurements.

2. Theory

The CTMC method was first applied to the study of ion–atom collisions by Abrines and Percival (1966a, b) as an adaptation of the Monte Carlo methods of Wall *et al* (1961) and Blais and Bunker (1962), and has been subsequently applied by a number of investigators. In brief, this technique is a simulation of a collision in which a large ensemble of initial electronic configurations is sampled in order to mimic the quantum mechanical position and momentum distributions, and therefore the wavefunction, of the atom. The subsequent motions of the projectile, target electron(s) and target core are then followed by solving the classical Hamilton equations for a sequence of time steps through the collision. After the particles have separated, knowledge of their positions and momenta allows the scattering angle and energy loss of the projectile, the ejection angle and energy of any free electrons and the binding energies and orbital angular momenta of any bound electrons to be determined in the asymptotic regime.

A number of variants of this basic model have been introduced, which differ, for example, in the interaction potentials used, additional terms in the Hamilton equations to simulate effects such as dynamical screening or Pauli exclusion, the type of initial distribution designed to represent different aspects of the quantum mechanical distributions and the number of electrons explicitly included in the model. In the present case we have chosen models which reflect a balance between the level of sophistication and the computational speed of the specific methods, due to the very large number of trajectories required for calculating doubly differential cross sections. This has also lead to the choice of impact energy to study, namely 100 eV, since it is near the peak of the total ionization cross section for these targets and has been studied experimentally by several groups.

To simulate collisions with helium we have utilized the *n*-CTMC model (Olson 1988) in which both electrons are explicitly included in the equations of motion. Thus, the impinging projectile is scattered in the combined field of the target nucleus and the two electrons. Since the classical atom is unstable against autoionization when orbital electron–electron interactions are present, this interaction is ignored and each orbital electron is bound by an energy equal to the first ionization potential of helium. Thus, this model is largely analogous to the independent electron model (Hansteen and Mosebekk 1972, McGuire and Weaver 1977) concerning the resulting total ionization probabilities, but differing from it in that the particle trajectories will be influenced by the interaction of the projectile with both the orbital electrons.

For comparison, we have also performed calculations in which only one electron is explicitly included. In this case, a model potential is utilized to simulate the

position-dependent screening the projectile and orbital electron experience due to the presence of the second orbital electron. The independent electron model is then used to compute the probabilities, and therefore we refer to this model as CTMC-IEM. This model has been used extensively for heavy-particle impact and specifically for ionization doubly differential cross sections by, for example, Reinhold and Olson (1989).

The model we use for molecular hydrogen has been described by Meng *et al* (1989) and is an n-CTMC model in which not only have both orbital electrons been included explicitly in the equations of motion, but also both nuclei. The primary development in this case has been the method of generating the initial conditions to model the H_2 wavefunction. In the original application of this model the computation was simplified somewhat by assuming a straightline projectile trajectory. While this approximation is very good for intermediate energy heavy-particle–atom collisions, in electron impact the projectile can be greatly deflected and accelerated in the collision and we have therefore removed this restriction. In all of these models, electron exchange is included explicitly through the possibility of classical interchange.

Concerning the numerical effort required to obtain the doubly differential cross sections presented below, three million trajectories were calculated in each case for electron and positron impact of helium using the CTMC-IEM model. The computer code for this model is highly vectorized and optimized to run on CRAY architecture machines. The n-CTMC codes, however, have a serious numerical disadvantage because of the presence of two explicit electrons. Due to the post-collisional Coulomb interaction of the free particles after an ionizing collision, the trajectories must be integrated to very large distances. In the n-CTMC case, if only one electron is removed from the atom, single removal dominating double removal here, one electron remains in orbit about the target core, requiring much greater numerical effort (i.e. smaller time steps) to follow than the ejected electron. To partially alleviate this problem we have frozen the target core by reducing the number of equations to integrate after an orbital electron and the projectile have escaped to a sufficient (typically 100 au) distance and then allowed the increase of the size of the integration time step. After this the free particle trajectories are integrated to several tens of thousands of au before the final angles and energies are determined. Tests have been made to insure the proper distance at which the frozen core approximation may be made and what final distances are required to accurately obtain the asymptotic angles and energies. With this aid, the computation of approximately one million trajectories for each of the n-CTMC runs was possible (e + He, ē + He, e + H_2 and ē + H_2).

3. Ionization total cross sections: e, ē + H, H_2, He

To serve as a general basis of comparison between the theoretical models and experiment we have calculated the total cross section for ionization of H, H_2 and He by electron and positron impact using the models described above. The results are displayed in figure 1 along with experimental measurements representative of the best available for each collision system. In general the models reproduce well the trend of the measurements and their magnitude. The most obvious deviation is the fact that, as has been noted often before, the classical ionization cross sections decrease as E^{-1}, rather than as the quantum mechanically correct $E^{-1}\ln E$, for collision energies E larger than those where the cross section peaks. The agreement

with the experimental measurements is somewhat remarkable considering that the only quantum information in the model is that contained in the initial distribution of atomic orbitals.

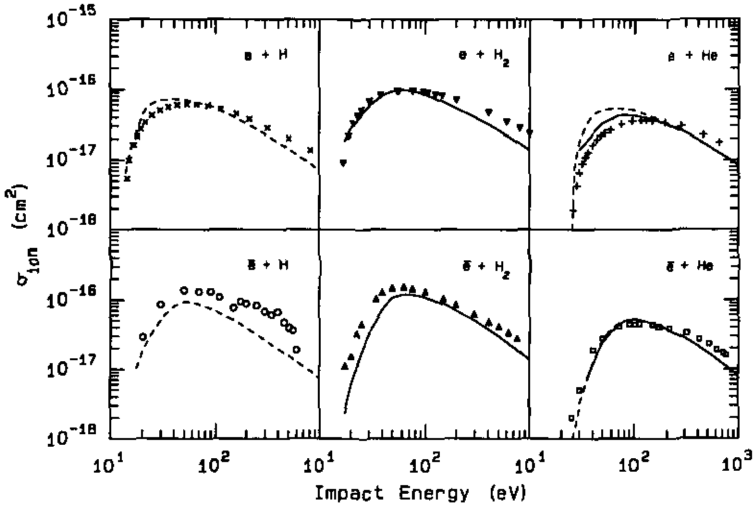

Figure 1. The total cross section for ionization of H, H_2 and He by electron and positron impact. Theoretical results are indicated by the full (n-CTMC) and broken (CTMC-IEM) curves. The experimental data are from Shah *et al* (1987) (e + H, ×, ± 8–12%), Rapp and Englander-Golden (1965) (e + H_2, ∇, ± 5%), Montague *et al* (1984) (e + He, +, ± 5%), Spicher *et al* (1990) (ē + H, ○, ± 15%), Knudsen *et al* (1990) (ē + H_2, Δ, ± 100% near threshold, 2–10% above) and Fromme *et al* (1988) (ē + He, □, ± 50% near threshold, 5–10% above). Approximate, typical experimental uncertainties are indicated here and in the subsequent figures by numbers in parentheses, determined by the present authors from the stated references.

The figure also indicates a significant difference between the n-CTMC and CTMC-IEM total cross sections for electron impact of helium in the lower half of the energy range displayed. This difference comes about due to collision events in which one of the orbital electrons, through its interaction with the projectile, becomes significantly more deeply bound than it was initially. This may occur because the classical atom has no minimum energy for the ground state. When such a transition occurs, the energy is conserved by a transfer of kinetic energy to the projectile. With this redistribution of energy the probability of ionization is changed. This effect is especially significant near ionization threshold and therefore the slope of the total cross section as threshold is approached is much different to the CTMC-IEM model. Such events are not reflected by the CTMC-IEM cross section, since they require not only a drop in binding energy of an electron with the accompanying transfer of energy to the projectile, but also the presence of another free electron for the event to be observed as ionization.

Events such as these which can be associated with the strong interaction of the projectile with both the target electrons are probably real in origin, but the lack of the minimum ground state binding energy in the classical models allows energy transfers to occur which violate quantum mechanics. In heavy-particle impact ionization, such

energy transfers contribute negligibly to the kinetic energy of the projectile and manifestations of this problem are not observed. Similarly, for higher energy light-particle impact, the non-quantum energy transfers are less important and the n-CTMC and CTMC-IEM results converge since otherwise they are equivalent expressions of the independent electron model regarding total ionization probabilities. Positron impact events in the n-CTMC model also show a contribution from this process but it is smaller in magnitude because the opposite charge sign of the projectile suppresses, to some extent, the 'pushing' of the orbital electron to lower energy. The stability of the quantum mechanical atom under electron–electron interactions due to the Heisenberg uncertainty principle is an essential feature which preliminary development of a more elaborate CTMC model has sought, in another context, to include (see e.g. Kirschbaum and Wilets 1980). Consequences of this behaviour of the n-CTMC model for light-particle impact are seen in the differential cross sections discussed below.

4. Ionization singly differential cross sections: e, ē + He, H_2

The singly differential cross section (SDCS) as a function of electron angle and energy for 100 eV electron impact of helium is displayed in figure 2, comparing the n-CTMC and CTMC-IEM results with the experimental measurements of Rudd and DuBois (1977). It is interesting to note that even though the projectile electron has a deBroglie wavelength differing only by a factor of about two from that of the atomic electrons, the classical model of their interaction still provides a reasonably good representation of the singly differential cross sections. Regarding the angular distribution, the n-CTMC and CTMC-IEM results both agree fairly well with the data, but differ in the detailed shape of the cross section they predict, especially for angles greater than ninety degrees.

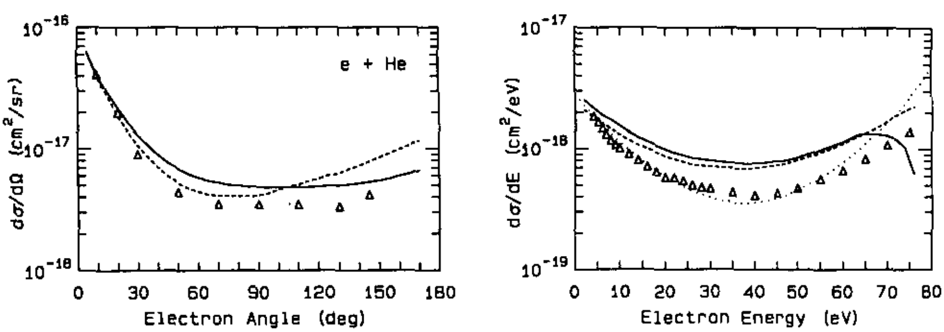

Figure 2. The singly differential cross section for the ionization of helium by 100 eV electron impact as a function of electron angle and energy. Theoretical results are indicated by the full (n-CTMC) and broken (CTMC-IEM) curves. Also included is the semiempirical fit given by Rudd (1991). The experimental data are from DuBois and Rudd (1978) (Δ, ± 20%).

The behaviour to be expected of the energy distribution of electrons is constrained by the fact that energy must be conserved. That is, if the incident energy is E_0, then

the most energetic electron which can be produced in the ionization process has an energy $E_0 - I$, where I is the ionization potential. For a helium target this maximum energy is 100−24.59=75.41 eV (85.6 eV for H_2). In this impact energy regime single ionization is much more likely than double ionization so, to a good approximation, for every electron of energy E, there must be another electron of energy $E_0 - I - E$. Thus, the energy spectrum is roughly symmetric about the energy $E_s = (E_0 - I)/2$ = 37.7 eV (42.3 eV for H_2).

This is reflected by the experimental data and the CTMC-IEM result, but is not reproduced at high electron energies by the n-CTMC model for which a roll-off is observed. This situation arises due to the problem associated with the non-quantum transfer of energy to the projectile when an orbital electron drops to a too low energy state of the classical atom. Thus, the lack of a minimum classical binding energy level allows electrons to obtain energies larger than quantum mechanically possible. The energy distribution drops at large electron energies because the flux of ejected electrons is spread to too high energies. As noted above, a more elaborate model in which the electrons were constrained in order to allow their mutual interaction would be required not only to insure stability against unphysical autoionization, but also to prevent this unphysical energy transfer.

Presented for reference in this figure and subsequent figures where appropriate are the semiempirical fits given by Rudd (1991). Rudd determined functional forms for the SDCS and doubly differential cross sections for the ionization of He and H_2 by electron impact, which have been designed to be consistent not only with all experimental measurements available but also with certain theoretical requirements. This work follows an earlier effort by Kim (1983) to produce recommended values for these cross sections.

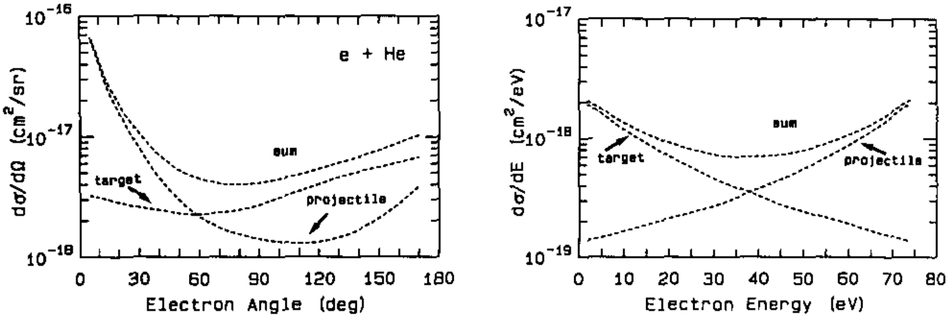

Figure 3. The singly differential cross section for the ionization of helium by 100 eV electron impact as a function of electron angle and energy. The broken curves indicate the CTMC-IEM result divided into projectile electron and target electron contributions to their sum.

Since the projectile and target electrons are classically distinguishable, in figure 3 we divide the yield of electrons into the target and projectile contributions obtained from the CTMC-IEM model. We see that the forward peak is composed, as would be expected, mostly of projectile electrons and that the target electrons are ejected more isotropically, with some enhancement in the backward direction. This occurs due

to the post-collisional electron–electron repulsion. That is, the projectile electrons, which are primarily scattered into the forward direction have a long range repulsive interaction with the nearly isotropically ejected target electrons, pushing them to larger angles as they escape into the asymptotic regime. Also noted is a backward peak in the projectile scattering arising from very close encounters with the nucleus. Consequently the sum of the projectile and target electron contributions shows a strong forward peak and a smaller backward enhancement from the post-collisional interaction (PCI) and the backscattered projectiles, superimposed on an isotropic background.

Similarly the energy spectrum shows that the target electron distribution is peaked at very low ejected electron energies, while the projectile contribution is peaked at the highest energies consistent with energy conservation, the two curves crossing at the symmetry point E_s. Thus, as expected, collisions in which the target electron is just barely removed and the projectile loses only a small amount of energy in excess of the ionization potential are dominant.

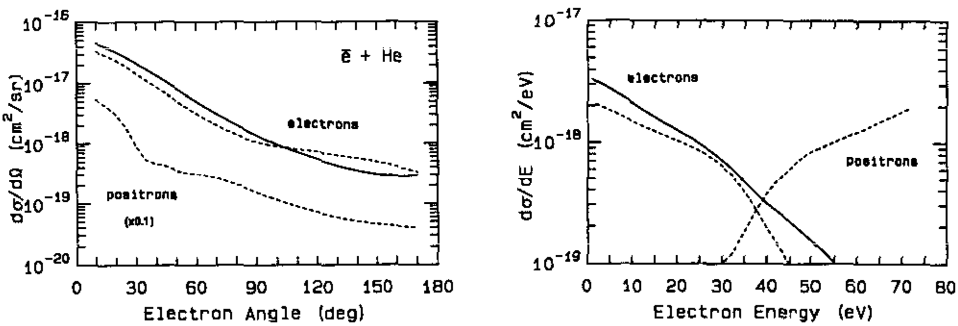

Figure 4. The singly differential cross section for the ionization of helium by 100 eV positron impact as a function of electron (or positron) angle and energy. The broken curves indicate the CTMC-IEM result for the ejected electrons and the scattered incident positrons and the full curve indicates the n-CTMC result for the ejected electrons.

If we consider collisions in which the projectile charge sign is reversed (i.e. positron impact), the SDCS display differences due to the change in the sign of the PCI and since the projectile is distinguishable from the ejected electrons. This is illustrated in figure 4 for 100 eV positron impact of helium. In this case, the shape of the SDCS as a function of angle is similar to that obtained in the electron impact case, but the difference in magnitude of the cross section in the forward and backward directions is much larger. In the electron impact case the decline of the SDCS from forward to backward angles is about a factor of ten whereas for positron impact the drop is twice as large. For positrons the projectile–ejected-electron interaction is attractive and consequently the electrons tend to be focused by the PCI into the forward direction since, as also indicated in the figure, the positrons are primarily forwardly scattered. The curve in this figure indicating the distribution of the positron scattering angles detected in coincidence with ionization shows the forward peak due to scattering from the electrons and then at about thirty degrees a change in slope indicating the wider angle deflections due to scattering from the nucleus.

The energy distribution is very similar to that found for electron impact but here the cross section drops monotonically with increasing electron energy since the projectile contribution is absent. The two energy single differentials (for ejected electrons and for scattered positrons) intersect again near the symmetry energy E_s.

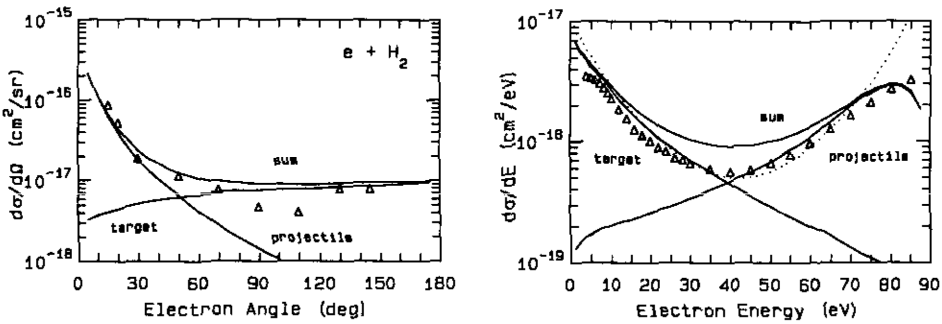

Figure 5. The singly differential cross section for the ionization of molecular hydrogen by 100 eV electron impact as a function of electron angle and energy. The full curves indicate the n-CTMC result divided into the projectile electron and target electron contributions to their sum. The dotted curve indicates the semiempirical fit of Rudd (1991). The experimental data are from Rudd and DuBois (1977) (Δ, ± 20%).

Comparison of the n-CTMC results for 100 eV electron impact of H_2 with the measurements of DuBois and Rudd (1978) is presented in figure 5, and is found to be quite similar to the same comparison for electron impact of He. The magnitude of the singly differential cross section for collisions with H_2 is slightly larger than for He owing to the difference in ionization potentials. Again the CTMC model reproduces well the forward peak of the angular distribution of electrons and its flattening out at larger angles. As in the n-CTMC treatment of helium the unphysical energy transfers cause the roll-over of the high energy portion of the ejected electron spectrum, but the rest of the shape is reasonably represented. The angular distribution of target electrons is again mostly isotropic, with the repulsive PCI biasing the electrons somewhat towards the backward direction. It may be noted that with both He and H_2 targets the largest contribution to the CTMC model's overestimation of the total yield of electrons comes from near energy sharing collisions. That is, the CTMC SDCS as a function of electron energy is about a factor of two too large near E_s but agrees much better for small or large electron energies.

The results for positron impact of H_2, illustrated in figure 6, are also quite similar to those for positron impact of He. In particular, the shape of the SDCSs are largely the same as in the case of helium, the overall magnitude being somewhat larger due to the difference in ionization potentials noted above. In rough terms, the difference in magnitude is the ratio of the ionization potentials, a factor of about 1.6, but the H_2 cross sections are larger by as much as a factor of three in some angle and energy ranges. As may also be noted from this figure, the n-CTMC model displays the same type of roll-over at high energies that it did for electron impact. This occurs due to a similar mechanism in which the positron carries away an extra amount of energy gained when one of the orbital electrons drops to a too tightly bound state during the collision.

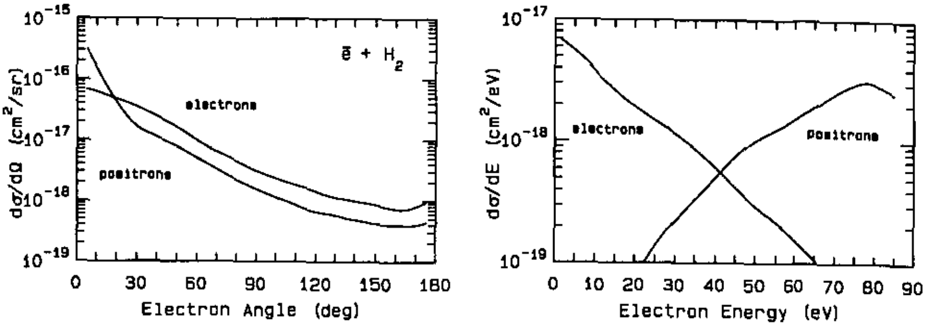

Figure 6. The singly differential cross section for the ionization of molecular hydrogen by 100 eV positron impact as a function of the electron (or positron) angle and energy. The full curves indicate the n-CTMC result for the ejected electrons and the scattered incident positrons.

Thus, the major features of the singly differential cross sections for electron impact of He and H_2 are reproduced by the classical models, and reasonable agreement with experimental measurements in shape and magnitude is obtained. Differences in the SDCS when the sign of the projectile charge is reversed are manifested by the difference from a repulsive to attractive PCI and due to the distinguishability of the projectiles from the ejected electrons in this case. Manifestations of the differences in ionization mechanisms due to the charge sign reversal have been discussed at length elsewhere (see Schultz *et al* 1991). Also, the problem of non-quantum energy transfer to the projectile accompanying ionization in the n-CTMC model of light-particle impact have been identified and their consequences noted. Clearly, the improved dynamical representation of the projectile scattering from the composite target in the n-CTMC model over the CTMC-IEM case is offset by this shortcoming and a more elaborate model in which the electron–electron repulsion was constrained would be a very useful future avenue to explore.

5. Ionization doubly differential cross sections: e, ē + He, H_2

Just as consideration of the SDCS presents a more stringent test of a theoretical model than does the total cross section alone, comparison with experimental measurements of the doubly differential cross section (DDCS) allows an even more detailed appraisal of the present model's merits and limitations. Consequently, we present in the remaining figures DDCSs for 100 eV electron and positron impact of He and H_2 compared to available experimental data and perturbative quantum mechanical theory. In each case we display the cross section as a function of electron angle for several fixed electron energies.

For example, in figure 7 we present a comparison between four sets of experimental measurements and the results of the n-CTMC and CTMC-IEM calculations. The most recent data are those of Ehrhardt's group at Universität Kaiserslautern (Müller-Feidler *et al* 1986) and we note that Rudd's (1991) recommended fits typically lie closest to this data set. The other measurements (Opal *et al* 1972, Rudd and

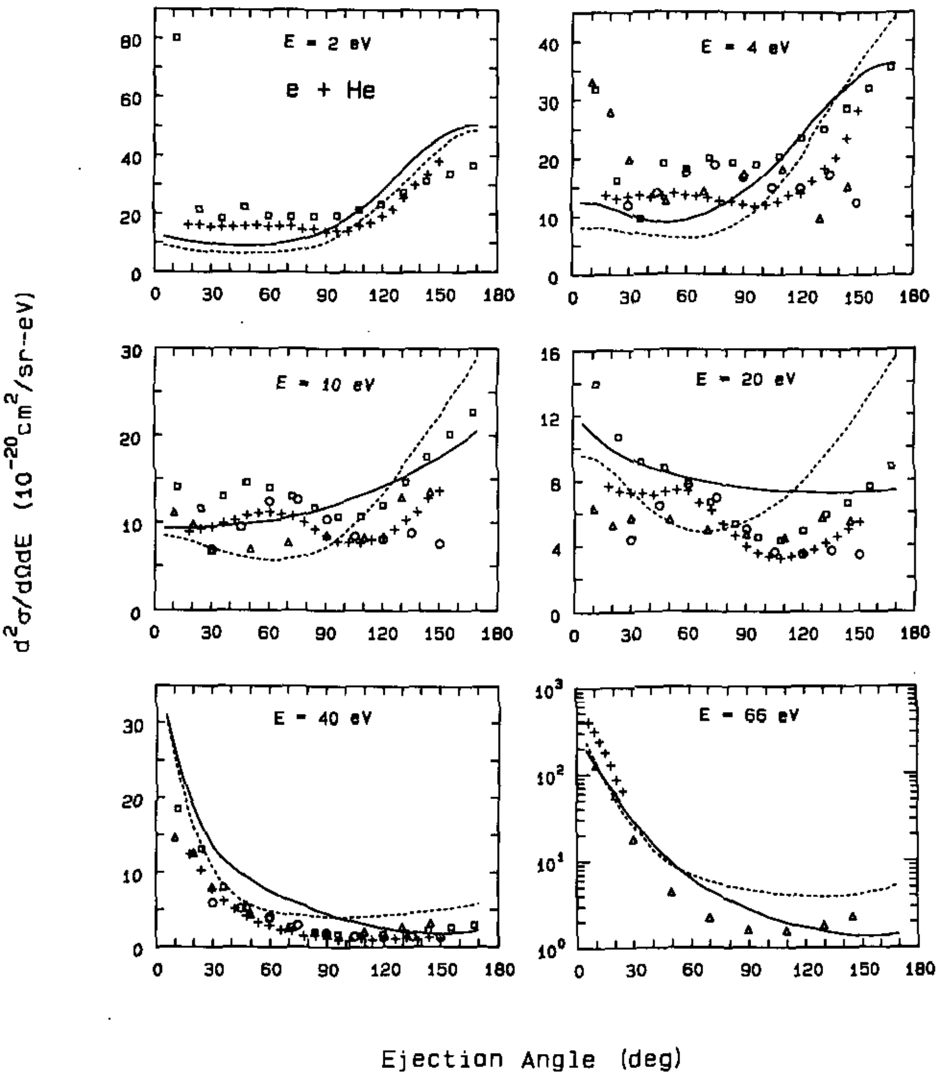

Figure 7. The doubly differential cross section for the ionization of helium by 100 eV electron impact as a function of electron angle for several electron energies. The theoretical results are indicated by the full (n-CTMC) and broken (CTMC-IEM) curves. The experimental data are from Müller-Fiedler *et al* (1986) (×, ± 5%), Shyn and Sharp (1979) (□, ± 17%), Rudd and DuBois (1977) (Δ, ± 20%) and Opal *et al* (1972) (O, ± 10%).

DuBois 1977, Shyn and Sharp 1979) show substantial agreement in some regimes but also show considerable differences, testifying to the difficulty of the experimental determination of these cross sections, and the reader is referred to the original works for discussion and analysis of the experimental uncertainties.

Inspection of this figure immediately indicates that the CTMC models reproduce the experimental shapes and magnitude best for either small or large electron

energies, a trend noted in our discussion of the SDCS. At electron energies of 2 and 4 eV, for example, the electrons detected are almost entirely target electrons and, in this case, both the experiment and theory show the characteristic biasing toward backward angles due to the repulsive PCI with the forwardly scattered, faster projectile electrons. Also, for large electron energies, in which case the detected electrons are primarily projectile electrons, the strongly forwardly peaked distribution is well reproduced by the models. However, at intermediate electron energies, the measurements exhibit a more complicated shape. The CTMC cross sections are comprised of a nearly direct superposition of the typical projectile (forwardly peaked) and target (backwardly peaked) electron distributions, yielding results intermediate to the small and large electron energy cases.

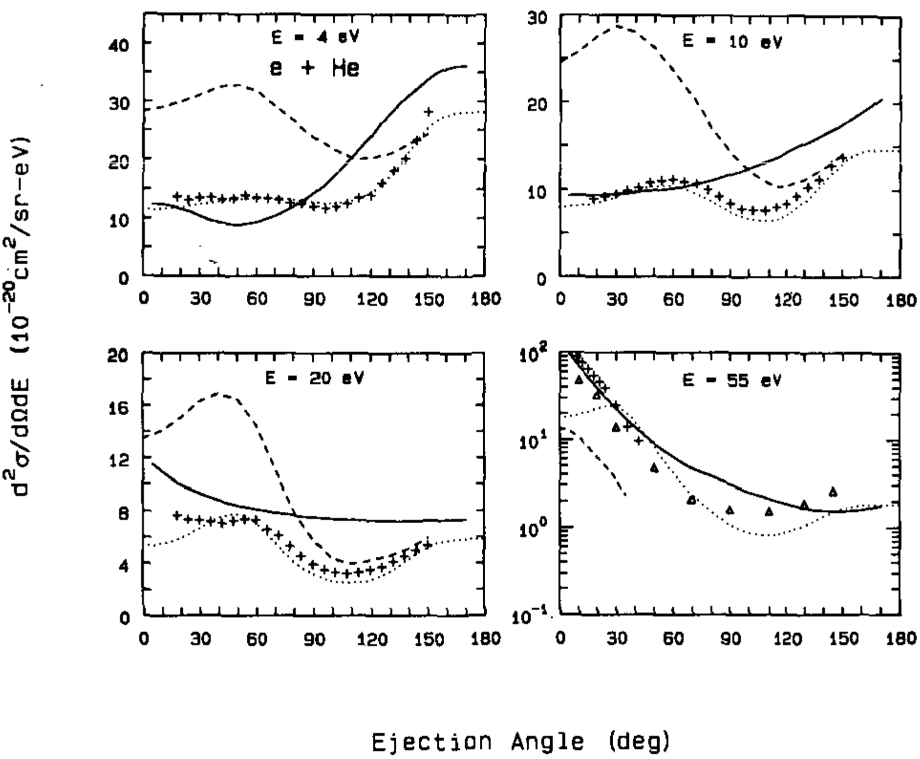

Figure 8. The doubly differential cross section for the ionization of helium by 100 eV electron impact as a function of electron angle for several electron energies. The n-CTMC (full curves) results are compared to the distorted-wave Born approximation of McCarthy and Zhang (1989) (broken curves), the semiempirical fit of Rudd (1991) (dotted curves) and the experimental data of Müller-Fiedler *et al* (1986) (+, ± 5%).

Quantum mechanically, these more complicated shapes at intermediate electron energies come from the integration of peaks in the distributions aligned with the momentum transfer vector and at right angles to it. Such features can be recognized in figure 8 in which we compare the n-CTMC and distorted-wave Born approximation (DWBA) (McCarthy and Zhang 1989) results with the data of Müller-Feidler *et al*

(1986) and the recommended fit of Rudd (1991). An energy of 100 eV may be considered rather low for the assured validity of a perturbative treatment such as the DWBA, but we note that the distortion of the electronic wavefunction which it takes into account is usually assumed to approximate the inclusion of higher Born series terms and that the method is often applied at even lower energies, down to the ionization threshold. At intermediate energies, the DWBA is often the only quantum mechanical approximation used due to the difficulties associated with the large basis set required in close coupling. In the present case, for 4, 10 and 20 eV detected electrons, the DWBA theory has the oscillations present in the experimental measurements, but overestimates the magnitude of the cross section by amounts which vary with electron angle and energy. At 55 eV, the DWBA underestimates the SDCS by about a factor of ten.

However, such disagreements between quantum mechanical perturbative treatments and experiment regarding low to intermediate energy electron impact ionization have been noted for some time. Specifically, over more than the past decade, groups such as those as Universität Kaiserslautern have made detailed coincident measurements yielding the triply differential cross section (see e.g. Ehrhardt *et al* 1986, Schlemmer *et al* 1991). Much work has been done theoretically to try to explain the features of such measurements which differ from first-order Born and DWBA calculations, such as the computation of the second-order Born term, the use of classical PCI corrections and the explicit inclusion of an exit channel wavefunction which has the asymptotic form of three Coulomb waves representing the free particles in single ionization (see e.g. Klar *et al* 1986, Brauner *et al* 1989, Schlemmer *et al* 1991 and Curran *et al* 1991). In light of these studies, the most difficult aspect of the triply differential cross sections to take account of is the quantum mechanical representation of the final state composed of three free particles. The long-range nature of the Coulomb interaction makes it impossible to treat only the near collision regime since the subsequent PCI strongly modifies the result.

In these terms, the present classical models represent very well the long range interaction of the projectile with the target in the initial state (polarization) and the evolution of the free particle trajectories in the final state. The extent to which the wave mechanical details of the collision itself are represented can be judged from the present comparisons, which show that the classical models produce a distribution of electrons which are in effect averaged over the quantum features of the cross sections.

Evidence of the attractive PCI is seen for 100 eV positron impact of helium (figure 9) and molecular hydrogen (figure 11) in that a strong forward peaking of the distribution of ejected electrons is observed at all electron energies. In another work, an extensive CTMC calculation of the doubly differential cross section for the ionization of atomic hydrogen by positron impact (Schultz and Reinhold 1990) has shown the crucial role of the PCI in the formation of the electron capture to the continuum (ECC) and binary ridge structures and the differences they show compared to their analogues in heavy-particle impact. Finally, we note that similar to the result for electron impact of helium, figure 10 shows that for electron impact of molecular hydrogen, the strongest agreement occurs for small and large electron energies, while the inflections in the n-CTMC cross section for intermediate electron energies do not closely correspond to the experimental trends or the recommended DDCS. As in helium, the intermediate energy cross sections reflect a transition from a backwardly (target electrons) to forwardly (projectile electrons) peaked distribution as larger electron energies are considered.

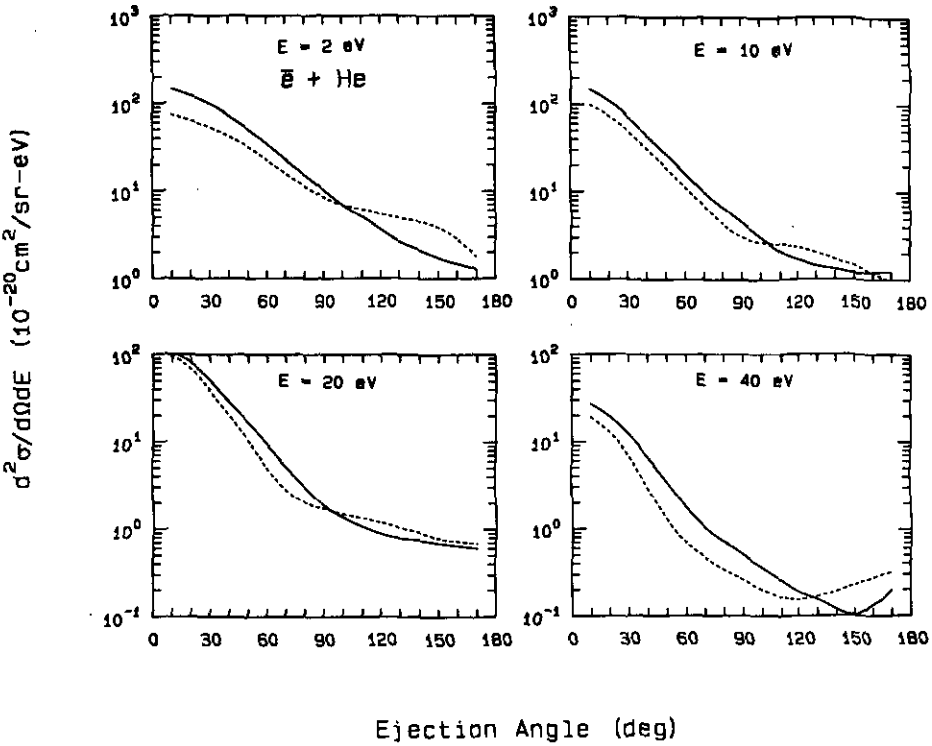

Figure 9. The doubly differential cross section for the ionization of helium by 100 eV positron impact as a function of electron angle for several electron energies. The theoretical results are indicated by the full (n-CTMC) and broken (CTMC-IEM) curves.

6. Conclusions

The present study has sought to explore the range of applicability of the the classical trajectory Monte Carlo technique to light-particle impact ionization of helium and molecular hydrogen. It has been shown that the classical model provides a reasonable description of the features of the singly and doubly differential cross sections for slow and fast electrons and where the effects of post-collisional interaction are important. In the intermediate range of electron energies, the method provides only rough agreement with experiment, representing an average between fast and slow electron behaviour rather than the more complicated structure evident experimentally and from quantum mechanical treatments. In addition, we have elucidate some of the most serious shortcomings of the model beyond the obvious lack of quantum wave-mechanical effects. In particular, when an n-CTMC approach is taken where both non-interacting orbital electrons of helium or molecular hydrogen are explicitly included in the equations of motion, the spectrum of final electron energies can be significantly effected by the lack of a minimum ground energy level of the classical atom. This behaviour comes about when, accompanied by ionization, the projectile electron (or positron) interacts with an orbital electron, pushing it to an orbit lower in energy than present in the initial state and therefore gaining a non-quantum energy transfer.

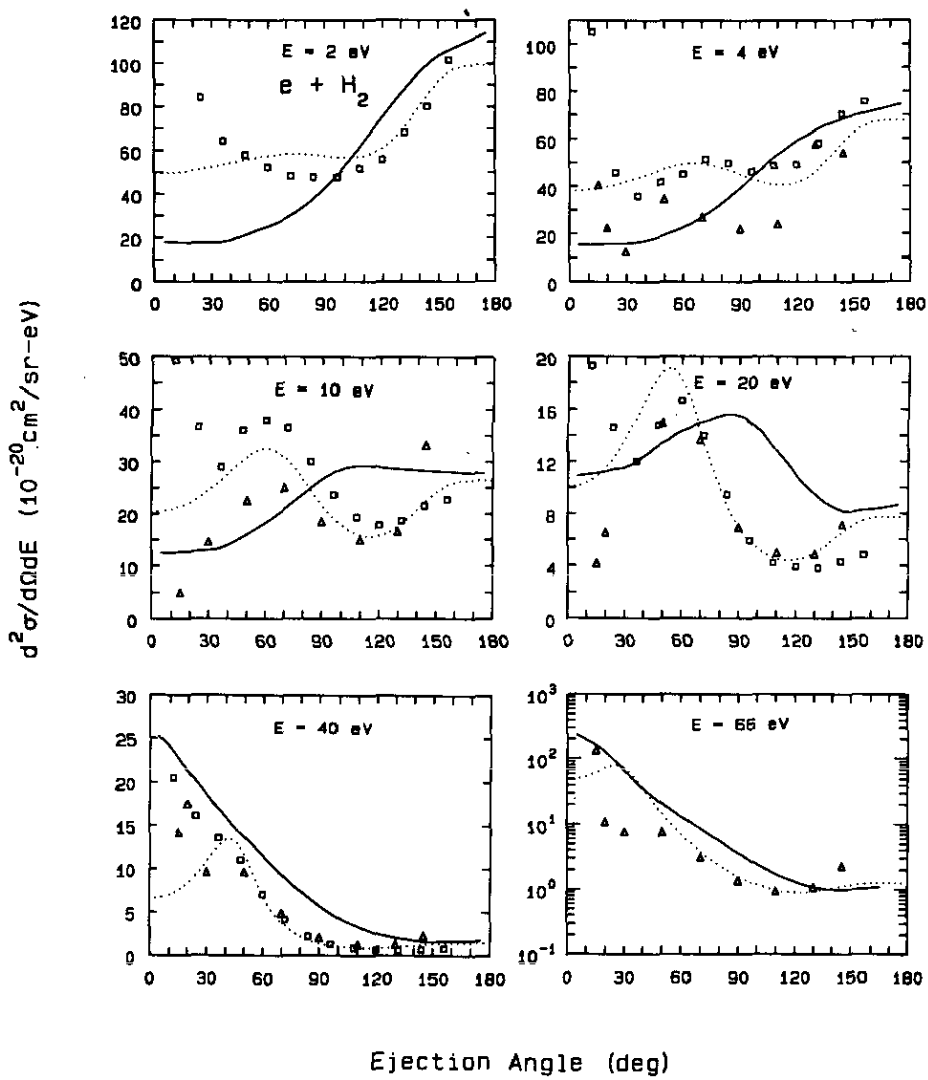

Figure 10. The doubly differential cross section for the ionization of molecular hydrogen by 100 eV electron impact as a function of electron angle for several electron energies. The n-CTMC (full curves) result is compared to the semiempirical fit of Rudd (1991) (dotted curves) and the experimental data of Shyn *et al* (1981) (□, ± 16%) and DuBois and Rudd (1978) (Δ, ± 20%).

This effect has also been noted in the energy dependence of the total ionization cross section near threshold. The CTMC-IEM results presented do not suffer to such a large extent from this problem since only one orbital electron is explicitly included and use is made of the independent electron model. A clear difference between use of the CTMC technique for light- and heavy-particle impact may be drawn in this case. That is, the non-quantum energy transfers are significant for light projectiles since this may reflect a relatively large change in their kinetic energy whereas it

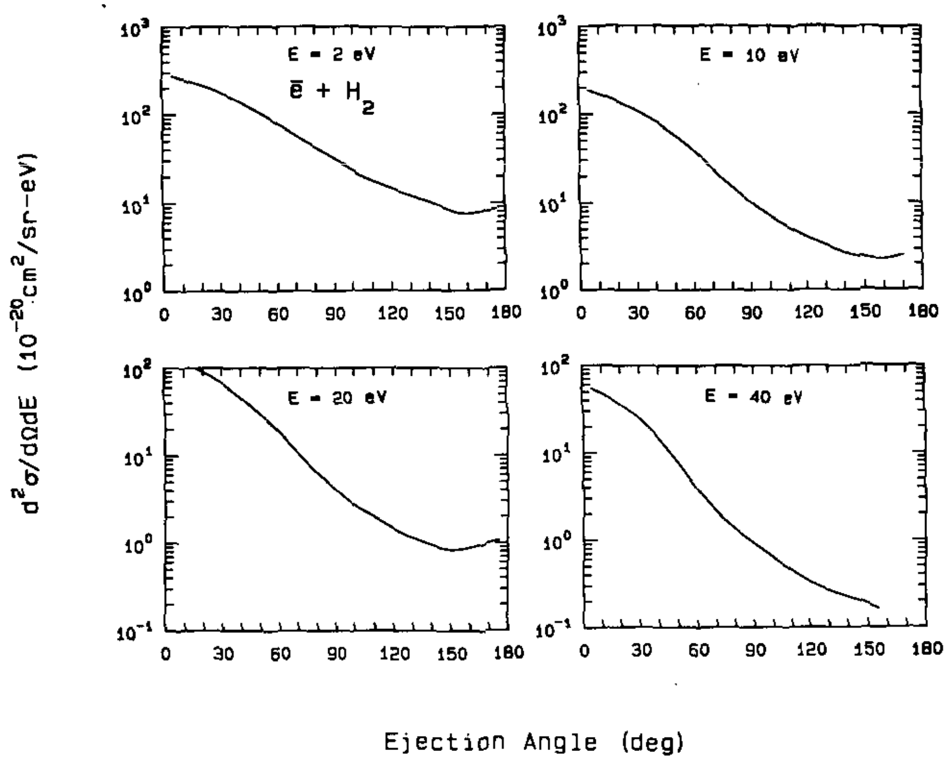

Figure 11. The doubly differential cross section for the ionization of molecular hydrogen by 100 eV positron impact as a function of electron angle for several electron energies. The n-CTMC result is indicated by the full curves.

is a negligible effect for a heavy projectile. Until a model for light-particle impact can be successfully applied which constrains the orbital electrons from such unphysical transitions, a problem closely related to the autoionization of the classical atom subject to orbital electron–electron interactions, the most reliable CTMC results from light-particle impact should come from application of the independent electron model and model potential or pseudopotentials representing the net effect of the other electrons.

Thus, the classical model has yielded results in perhaps surprisingly good agreement with experiment for 100 eV electron impact ionization. However, more elaborate models must be explored which can incorporate the leading quantum mechanical effects not present in this model based on classical particle trajectories. We have specifically underscored the effects that arise from quantum mechanical interactions with and among the orbital electrons in a multielectronic atom and which would have to be treated in a more complete model. In addition, proper account should be taken of the quantum effects such as tunnelling and the interference of trajectories with varying phases. Regarding these phenomena, extensive work in elastic scattering theory has historically shown that semiclassical treatments, such as the JWKB approximation, can reproduce the quantum features, but application of these ideas to the non-central, three-dimensional problem of electron impact has not,

to our knowledge, been reported and remains a challenge.

Acknowledgments

The authors would like to gratefully acknowledge the support of the Office of Fusion Research, US Department of Energy and one of us (DRS) acknowledges additional partial support from the US Department of Energy's Fusion Postdoctoral Fellowship program. Helpful conversations with Professor J Macek are also appreciatively acknowledged.

References

Abrines R and Percival I C 1966a *Proc. Phys. Soc.* **88** 861
—— 1966b *Proc. Phys. Soc.* **88** 873
Abrines R, Percival I C and Valentine N A 1966 *Proc. Phys. Soc.* **89** 515
Banks D and Boesten L G J 1978 *J. Phys. B: At. Mol. Phys.* **11** 2209
Blais D L and Bunker N C 1962 *J. Chem. Phys.* **37** 2713
Boesten L G J, Banks D and Heideman H G M 1976 *J. Phys. B: At. Mol. Phys.* **9** L97
Boesten L G J, Heideman H G M, Bonsen T F M and Banks D 1976 *J. Phys. B: At. Mol. Phys.* **9** L1
Brauner M, Briggs J S and Klar H 1989 *J. Phys. B: At. Mol. Opt. Phys.* **22** 2265
Charlton M and Laricchia G 1990 *J. Phys. B: At. Mol. Opt. Phys.* **23** 1045
Curran E P, Whelan C T and Walters H R J 1991 *J. Phys. B: At. Mol. Opt. Phys.* **24** L19
Dimitrijevic M S and Grujic P 1979 *J. Phys. B: At. Mol. Phys.* **12** 1873
—— 1983 *J. Phys. B: At. Mol. Phys.* **16** 297
DuBois R D and Rudd M E 1978 *Phys. Rev.* A **17** 843 and unpublished tables
Ehrhardt H, Jung K, Knoth G and Schlemmer P 1986 *Z. Phys.* D **1** 3
Fromme D, Kruse G, Raith W and Sinapius G 1988 *J. Phys. B: At. Mol. Opt. Phys.* **21** L261
Hansteen J M and Mosebekk O P 1972 *Phys. Rev. Lett.* **29** 1361
Kauppila W E and Stein T S 1989 *Adv. At. Mol. Opt. Phys.* **26** 1
Kim Y-K 1983 *Phys. Rev.* A **28** 656
Kirschbaum C L and Wilets L 1980 *Phys. Rev.* A **21** 834
Klar H, Franz A and Tenhagen H 1986 *Z. Phys.* B **1** 373
Knudsen H, Brun-Nielsen, Charlton M and Poulsen M R 1990 *J. Phys. B: At. Mol. Opt. Phys.* **23** 3955
McCarthy I E and Zhang X 1989 *J. Phys. B: At. Mol. Opt. Phys.* **22** 2189
McGuire J H and Weaver L 1977 *Phys. Rev.* A **16** 41
Meng L, Reinhold C O and Olson R E 1989 *Phys. Rev.* A **40** 3637
Montague R G, Harrison M F A and Smith A C H 1984 *J. Phys. B: At. Mol. Phys.* 17 3295
Müller-Fiedler R, Jung K and Ehrhardt H 1986 *J. Phys. B: At. Mol. Phys.* **19** 1211
Ohsaki A, Watanabe T, Nakanishi K and Iguchi K 1985 *Phys. Rev.* A **32** 2640
Olson R E 1988 *Electronic and Atomic Collisions* ed H B Gilbody, W R Newell, F H Read and A C H Smith (Amsterdam: Elsevier) p 271
Olson R E and Gay T J 1988 *Phys. Rev. Lett.* **61** 302
Opal C B, Beaty E C and Peterson W K 1972 *At. Data* **4** 209
Percival I C 1973 *J. Phys. B: At. Mol. Phys.* **6** 93
—— 1974 *Comput. Phys. Commun.* **6** 347
Percival I C and Richards D 1978 *Mon. Not. R. Astron. Soc.* **183** 329
Percival I C and Valentine N A 1967 *Proc. 5th Int. Conf. on Physics of Electronic and Atomic Collisions* (Leningrad: Nauka) Abstracts p 121
Rapp D and Englander-Golden P 1965 *J. Chem. Phys.* **43** 1464
Reinhold C O and Olson R E 1989 *Phys. Rev.* A **39** 3861
Rudd M E 1991 *Phys. Rev.* A **44** 1644
Rudd M E and DuBois R D 1977 *Phys. Rev.* A **16** 26 and unpublished tables
Schlemmer P, Srivastava M K, Rösel and Ehrhardt H 1991 *J. Phys. B: At. Mol. Opt. Phys.* **24** 2719
Schultz D R 1989 *Phys. Rev.* A **40** 2330

Schultz D R and Olson R E 1988 *Phys. Rev.* A **38** 1866
Schultz D R, Olson R E and Reinhold C O 1991 *J. Phys. B: At. Mol. Opt. Phys.* **24** 521
Schultz D R and Reinhold C O 1990 *J. Phys. B: At. Mol. Opt. Phys.* **23** L9
Schultz D R, Reinhold C O and Olson R E 1989 *Phys. Rev.* A **40** 4947
Shah M B, Elliott D S and Gilbody H B 1987 *J. Phys. B: At. Mol. Phys.* **20** 3501
Shyn T W 1992 *Phys. Rev.* A **45** 2951
Shyn T W and Sharp W E 1979 *Phys. Rev.* A **19** 557
Shyn T W, Sharp W E and Kim Y-K 1981 *Phys. Rev.* A **24** 79
Spicher G, Olsson B, Raith W, Sinapius G and Sperber W 1990 *Phys. Rev. Lett.* **64** 1019
Wall F T, Hiller L A and Mazur J 1961 *J. Chem. Phys.* **35** 1284
Wetmore A E and Olson R E 1986 *Phys. Rev.* A **34** 2822